

Coalescence of Oil Droplets using Sponge-like Structure of Polyvinylidene Fluoride Membranes

C. K. Chiam*, M. Nurashiqin, K. Zykamilia, N. M. Ismail, K. Duduku & S. Rosalam

Membrane Technology Research Group, Material and Mineral Research Unit, Faculty of Engineering, Universiti Malaysia Sabah, Jalan UMS, 88400 Kota Kinabalu, Sabah, Malaysia

Submitted: 21/9/2018. Revised edition: 5/11/2018. Accepted: 6/11/2018. Available online: 5/12/2018

ABSTRACT

This work reports the effect of the membrane pore size distribution on the oil droplets size distribution in permeate using the polyvinylidene fluoride (PVDF) membranes. The sponge-like structures of the PVDF membranes were fabricated via the phase inversion technique using 30% v/v ethanol aqueous solution as coagulation medium. Water and polyethylene glycol (PEG1000) were used as the pore forming additives in the dope solutions. Microfiltration was employed to coalesce the oil droplets at the transmembrane pressure of 2.5 bar. Simulated alkaline-surfactant-polymer (ASP) produced water was tested as the feed solution. Results revealed that the PVDF membranes with sponge-like structure were formed. The additives in the dope solutions have induced the membranes to become thicker due to more porous, spongy and resilient structure. The membrane pore sizes increased with the presence of the additives in the dope solutions especially when larger molecular weight of the additive, i.e., PEG1000 was used. The mode of the oil droplets radius increased from 61.2 nm in the feed solution to 95.1, 356.2 and 1335 nm in the permeates by the corresponding membranes without additive, with water and PEG1000 as the additives. The membranes with larger pore sizes as well as more open structure were able to trap and coalesce more oil droplets which produced larger size of the oil droplets in the permeates.

Keywords: ASP produced water, PVDF membrane, sponge-like structure, microfiltration; coalescence

1.0 INTRODUCTION

Alkaline-Surfactant-Polymer (ASP) is a promising tertiary method for Enhanced Oil Recovery (EOR) which has been proven with an excellent oil recovery up to 98% of the original oil in place (OOIP) in laboratory tests [1]. The ASP flooding technology in EOR applied in Daqing oil field, China is the largest at the present time [2] with more than 15 years ASP testing for several pilots and different scales [3]. Other examples of the application of ASP EOR technology are Shengli and Karamay in China [4–5]; Taber South and Suffield in Canada; and West

Kiehl, Lawrence field Illinois and Cambridge Minnelusa in USA [6–8]. Nevertheless, the handling of the produced water from ASP process is challenging because the large volume and the chemical residuals contained in the produced water are hardly separated. The surfactant helps to stabilize the oil droplets by reducing the oil-water interfacial tension and zeta potential on the surfaces of the oil droplets. The skin barrier surrounding the tiny droplets in the oil-water emulsion prevents the oil droplets from uniting. Hence, the presence of the surfactant causes the produced water from ASP flooding becomes more

* Corresponding to: C. K. Chiam (email: chiamchelken@ums.edu.my)

complex and stable [9].

The management of the produced water becomes more challenging if it involves the offshore ASP EOR projects. Construction of the disposal wells for the wastewater is unfavorable as it is expensive. Overboard disposal is commonly practiced especially for the remote offshore locations. However, de-oiling is a difficult work because of the stringent regulatory standards for discharging produced water. For instance, the permitted oil and grease limits for treated produced water discharge offshore in China, Australia, US and North-East Atlantic range between 10 and 50 mg/L [10]. For the purpose of sustainability, reuse of the produced water for re-injection is an attractive option for offshore ASP EOR as this can reduce the environmental issue and lower the cost of chemicals. The crude oil that emulsified in the produced water is valuable and worth to be recovered.

Microfiltration by using hydrophobic membranes have been successfully tested for destabilizing the oil-water emulsion [11–14]. The hypothetical mechanism of the oil droplet coalescence [12] is illustrated in Figure 1. The surfactant films covered the oil droplets prevent the oil droplets from uniting in the feed. The feed contains the oil droplets is brought into a direct contact with the membrane surface. The oil droplets tend to attach on the membrane surface when the membrane surface is hydrophobic. The oil droplet deformed and squeezed into the membrane pore when the feed is pressurized. The surfactant film is stripped off and collapsed when the oil droplet is forced to flow into the narrow pore. Thus, the oil droplet is destabilized and coalescence happening when two

droplets without the surfactant films collide together. The coalesced oil droplets grow when they flow out from the membrane pore on the downstream side of the membrane.

Hydrophobic membranes such as polytetrafluoroethylene (PTFE) with various pore sizes are normally tested for destabilizing the oil droplets. Unno *et al.* [11] reported that the oil separation rate increased with the membrane pore size increased from 1 to 10 μm . Hlavacek [12] revealed that the oil droplet size distribution in permeate showed the peak about 100 μm while the initial mean droplet size was 1.8 μm by using the polypropylene (PP) hollow fiber membrane with the pore size of 0.2 μm . However, enlargement on the oil droplets was not significant when PP with effective pore size 0.05 μm was used for initial oil droplet size distribution from approximately 5 to 10 μm [13], while the larger pore size of the PTFE membrane, i.e., 5 μm was able to enlarge the oil droplet sizes from the initial droplet sizes less than 2 μm [15]. From the findings in the literature, the effect of membrane pore size on the oil droplet coalescence becomes significant if the membrane pore size exceeds 0.2 μm while smaller pore size, e.g., 0.05 μm has no essential effect on the coalescence. However, the effect of the membrane pore size on the oil droplets coalescence is not clear because in fact, the membrane pore size may distribute from 0.05 to 10 μm . Furthermore, the structures of the commercial membranes tested in the literature are not consistent. For instance, in reality, the membrane structure is tortuous instead of a straight cylindrical shape as shown in Figure 1 [12–14].

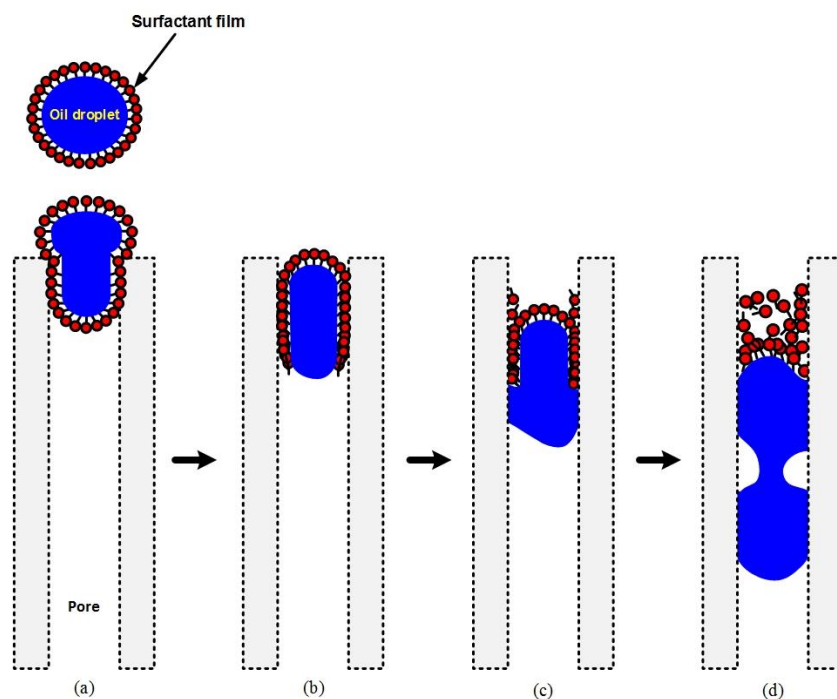


Figure 1 Hypothetical oil droplet coalescence through membrane permeation: (a) deformation (b) squeezing (c) surfactant film collapsing (d) coalescence and growing

This work aims to gain a better understanding for the effect of the membrane pore size distribution on the oil droplets coalescence by using a consistent membrane structure i.e. sponge-like structure. In order to obtain the sponge-like structure membranes with different pore size distributions, phase inversion technique is employed to fabricate the membranes from polyvinylidene fluoride (PVDF) and coagulated in a 30% v/v ethanol solution bath.

2.0 METHODS

2.1 Membrane Fabrication

Polyvinylidene fluoride supplied by Sigma–Aldrich in pellet form, was used to fabricate the membranes. *N,N*-dimethylacetamide (DMA) supplied by Acros Organics, was used the polymer solvent. Polyethylene glycol with molecular weight M_w 1000 purchased from Fluka, and distilled

water were used as the dope solution additives.

The compositions of the dope solution formulation were shown in Table 1. The appropriate amounts of the chemicals were mixed in a closed-bottle and stirred continuously on a hot plate at 50°C for 6 hours for producing a homogeneous solution. The dope solution was remained in a cabinet for three days for bubbles removal. The dope solution was poured carefully onto a clean and smooth glass plate; and immediately the solution was cast by using a knife at room temperature. Adhesive tape with thickness about 400 μm was placed at the edges of the glass plate for controlling the thickness of casting. The glass plate with the casted film was promptly immersed into a 30% v/v ethanol solution coagulation bath for 5 s and next into a water bath for 4 hours. The membranes were washed thoroughly with distilled water and then air-dried overnight at 23°C.

Table 1 Dope formulation for membranes

Membrane	Formulation (wt.%)	
PVDF1	PVDF/DMA	: 10/90
PVDF2	PVDF/DMA/water	: 10/88/2
PVDF3	PVDF/DMA/PEG solution*	: 10/88/2

* The PEG solution consists of 16.5 wt.% PEG and 83.5 wt.% distilled water.

2.1 Membrane Characterization

2.2.1 Membrane Structural Morphology

The structural morphology of the membranes was observed by using the scanning electron microscopy (SEM, Hitachi, S-3400N) after the membrane samples were fractured in the liquid nitrogen and sputter-coated with a thin gold film.

2.2.2 Thickness Measurement

The membrane thickness was measured by using a digital micrometer (RS 705-1229, China), with precision ± 0.001 mm, at 30 locations of the membranes, and its average value and the standard deviation were calculated.

2.2.3 Porosity Measurement

The membrane porosity is defined as the volume of the pores divided by the total volume of the membrane. Gravimetric method was used to determine the porosity of membranes. Isopropyl alcohol (Merck) was employed to wet the membrane pores. First, the dried membrane was immersed in the isopropyl alcohol for 30 minutes. The isopropyl alcohol entered the filled all the membrane pores. Next, the wetted membrane was immediately transferred into a distilled water bath and the membrane was immersed for another 30 minutes. The isopropyl alcohol diffused out from the

pores and dissolved in the water. The water replace the isopropyl alcohol inside the membrane pores. After 30 minutes, the membrane was immersed in a new water bath and rinsed. The excess water droplets on the membrane surfaces were removed by using a paper tissue. The membrane was weighted. The porosity of the membrane was determined as follows:

$$\varepsilon = \frac{100(w_w - w_d)/\rho_{\text{water}}}{(w_w - w_d)/\rho_{\text{water}} + w_d/\rho_{\text{PVDF}}} \quad (1)$$

where w_w is the wet membrane weight, w_d is the dry membrane weight, ρ_{water} is the water density (0.997 g/cm^3 at 25°C) and ρ_{PVDF} is the PVDF density (1.78 g/cm^3).

2.2.4 Pore Size Measurement

The membrane pore sizes were measured directly by using the SEM (Hitachi, S-3400N). The cross-section images of the membranes were observed at 10.0 kV of potential with magnifications of 6500x. The sizes of 100 membrane pores were randomly selected and measured for each membrane formulation.

2.3 Microfiltration Experiments

2.3.1 ASP Solution Preparation

A volume of 1 L of mineral water was prepared by using distilled water with the addition of 1600 mg/L NaCl; 2600 mg/L NaHCO₃; 300 mg/L Na₂CO₃; 40 mg/L Na₂SO₄; 40 mg/L CaCl₂ and 40

mg/L $MgCl_2$. To synthesize the oily wastewater produced from alkaline-surfactant-polymer (ASP) flooding, 1500 mg/L crude oil, 350 mg/L sodium dodecylbenzene sulphonate, 800 mg/L sodium hydroxide and 400 mg/L polyacrylamide were added into 996.95 g of the mineral water. The mixture in a cap-bottle was placed into a shaker with water bath temperature at 45°C and mixing rate at 120 rpm for 1 h.

2.3.2 Filtration Setup

A microfiltration as shown in Figure 2 purchased from Advanced Membrane Technology Research Center, Universiti Teknologi Malaysia, was employed to examine the coalescence of oil droplets. The membrane with an effective area of 17.35 cm² was placed into the permeation cell. The synthesized ASP produced water was placed in the feed tank. The feed was pumped into the permeation cell. The experiments were conducted at a constant feed flow rate of 1 L/min and transmembrane pressure of 2.5 bar. The permeate was collected into a beaker. The flux (J) was calculated as follows:

$$J = \frac{m}{At} \quad (2)$$

where m is the mass of permeate, A is the effective membrane area and t is the time of collecting the permeate.

2.3.3 Oil Droplet Size Analysis

A Malvern Zetasizer Nano ZS DLS Nano Zen 3600 which was a dynamic light scattering instrument was used to determine the sizes of the oil droplets in the feed water and permeate. The refractive index was 1.59 for the oil and 1.330 for the water.

3.0 RESULTS AND DISCUSSION

3.1 Membrane Properties

3.1.1 Morphology Study

SEM micrographs of the PVDF membranes coagulated in 30% v/v ethanol were shown in Figure 3. The PVDF membranes with sponge-like structure have been successfully produced by using the ethanol coagulation bath. Coagulation medium essentially influences the membrane formation during phase inversion process. The cross-section of the membrane morphology tends to become sponge-like structure when the coagulation rate is slower. In this work, the presence of the ethanol in the coagulation bath has reduced the water activity in the coagulation bath; thus, the diffusion of the DMA solvent as well as the additives into the coagulation bath is delayed and eventually sponge-like structure is formed. Similar observations have been found in the literature when ethanol is added in the coagulation baths [16–18].

3.1.2 Porosity

Table 2 presents the porosity of the PVDF membranes measured by using the Equation (1). Compared to the PVDF1 membranes, the additives in the dope solutions have increased the porosities in the PVDF2 and PVDF3 membranes. The membranes having the highest porosity when using PEG1000 as the additive. The family of PEGs has been known as the pore forming agents in membranes [19 – 20].

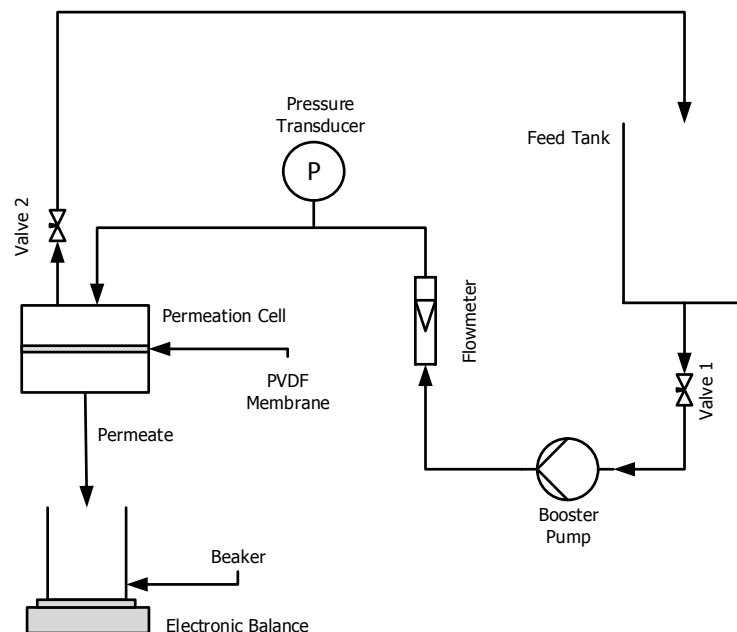


Figure 2 Microfiltration Setup

3.1.3 Thickness

The thickness of the membranes were measured by using the digital micrometre. The average thickness of the membranes is shown in the Table 2. Compared to the PVDF1 membranes, the thicknesses of PVDF2 and PVDF3 membranes are increased approximately 10 and 28% respectively. It is deduced that the dope solution additives have increased the membrane thickness by inducing more porous, spongy and resilient structure; the membrane porosity and thickness increase simultaneously as shown in Table 2.

3.1.4 Pore Size Distribution

The membrane pore sizes on the cross-sectional membranes were measured directly by using SEM. Figure 4 illustrates the pore size distribution of the PVDF membranes. The highest

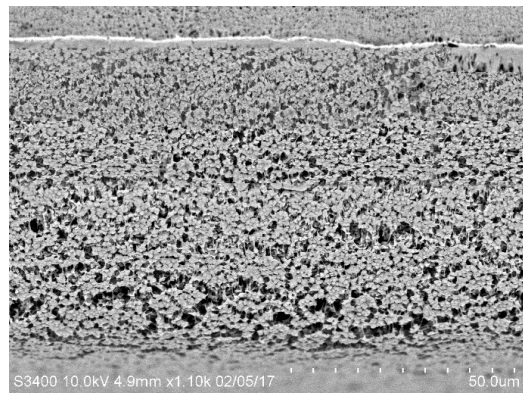
number of pores (peak) in PVDF1 membrane having the pore sizes between 0.30 and 0.90 μm which is about 40% of pores; in PVDF2 is between 0.90 and 1.50 μm which occupied by about 33%; while 28% of the pores in PVDF3 having sizes of 0.90 – 1.50 μm and 27% of the pores are within 1.50 – 2.10 μm . The membrane pore size becomes larger when additives are added in the dope solutions. The pores are formed when the additives diffused out from the thin film (dope solution) and mix into the coagulation bath. The distribution of the pore sizes in the PVDF3 is larger than that in the PVDF2; because the molecular weight of the additive used in the PVDF3 i.e. PEG1000 is larger than that of the additive used in the PVDF2 which is the water.

3.2 Coalescence of Oil Droplets

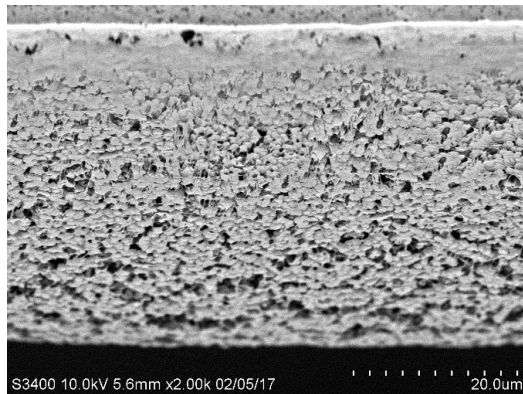
The permeation flux for each

Table 2 Membrane Properties

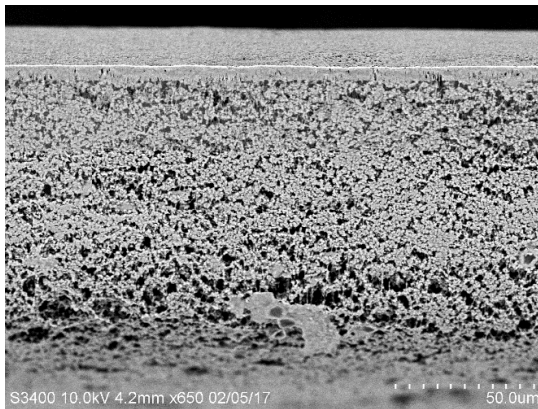
Membrane	Porosity (%)	Thickness (μm)	Morphology
PVDF1	48.2	98 \pm 6.6	Sponge-like
PVDF2	58.1	108 \pm 8.5	Sponge-like
PVDF3	63.6	126 \pm 4.8	Sponge-like



(a)



(b)



(c)

Figure 3 SEM images of the cross-section structures of the membranes, (a) PVDF1, (b) PVDF2 and (c) PVDF3

membrane formulation is determined by pressurizing the feed solution at 2.5 bar. Figure 5 shows the permeation fluxes for the membranes over time. By adding the additives in the membrane formulation solutions, the

fluxes increase in the order PVDF3 > PVDF2 > PVDF1 membranes. This indicates that the open pore structures on the membrane surface increase when adding water and PEG into the membrane dope solutions. The permeation fluxes values are in agreement with the data reported in Table 2 and Figure 4; that is, the membranes formulated from additives are spongier with larger porosity and more open pore structure as well as thickness increases. It is noteworthy that the effect of membrane thickness on the flux is lesser as compared to the effect of open pore structure.

The oil droplet sizes in the permeate were measured by using the dynamic light scattering instrument. Figure 6 exhibits the oil droplet size distribution in the permeate from the microfiltration through PVDF1, PVDF2 and PVDF3 membranes. Based on the statistical analysis, the mode of radius oil droplets in the feed ASP solution is 61.2 nm with intensity 25.8%. The mode of the radius of oil droplets in permeates increased to 95.1 nm by PVDF1, 356.2 nm by PVDF2 and 1335 nm by PVDF3 with the corresponding intensities 30.8, 22.1 and 28%. Compared to the oil droplets size distribution in the feed ASP produced water, the oil droplet sizes distributions are obviously shifted to the right of the graphs which indicated that the coalescence of the oil droplets occurred during the microfiltration process.

The oil droplet enlargement by the membranes is following the order PVDF3 > PVDF2 > PVDF1. A model of the oil droplet coalescence is thus developed as illustrated in Figure 7. The open pore structure increases in PVDF2 and PVDF3 membranes which may lead to the pore sizes exceeding the diameters of the oil droplets.

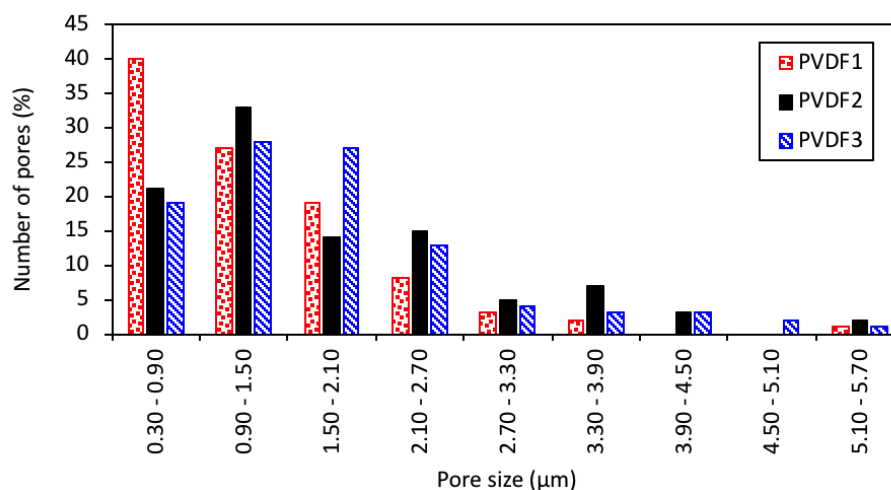


Figure 4 Pore size distribution of the cross-sectional membranes

Hence, the oil droplets will be trapped into the open pore structure at the membrane surface without deformation. Unlike the membrane pore structure shown in Figure 1 which is a straight cylindrical pores, in reality, the pores are tortuous in the sponge-like structure membranes. The oil droplets trapped in the pore membrane surface will be deformed, squeezed and flowed through the tortuous paths by the applied pressure and; eventually the surfactant films collapsed and the droplets combined to each other to become a larger droplet. The oil droplets in the feed channel are

easier to be escaped from the trapping into the pores due to the acting force from the cross-flow operation when the membrane with smaller open pore structure is used (Figure 7 (a)). Figure 7 (b) shows the larger open pore structure traps more oil droplets resulting in the larger coalesced oil droplets harvested in the permeate. Due to the coalescence of the more oil droplets occurred within the membrane pores, the permeation fluxes for the PVDF2 and PVDF3 are visibly reduced with time as shown in Figure 5.

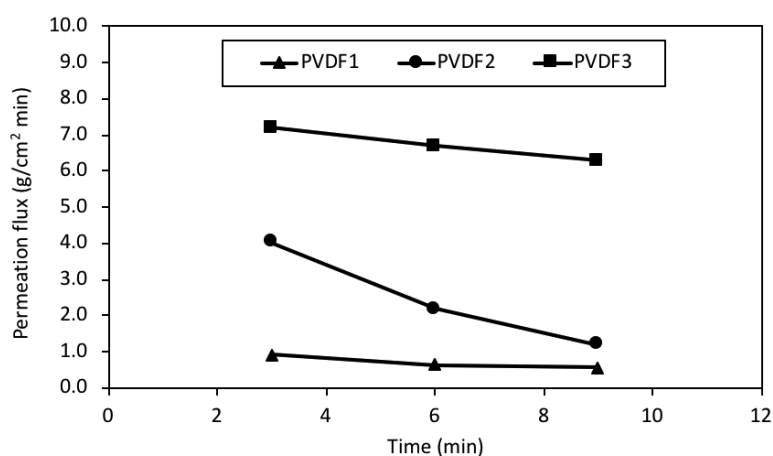


Figure 5 Microfiltration permeation fluxes as function of time at transmembrane pressure 2.5 bar

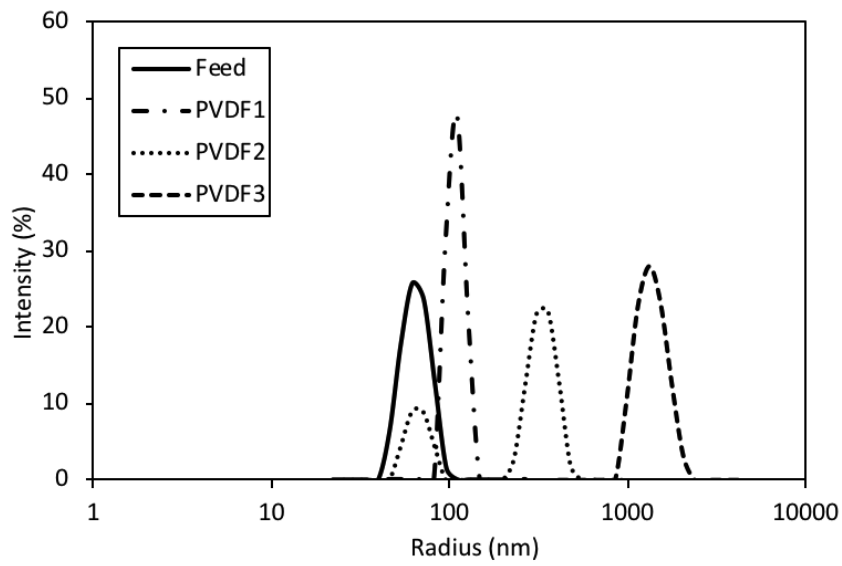


Figure 6 The distribution of the oil droplet size (radius) by intensity (%) in the feed ASP solution and permeates through the membranes

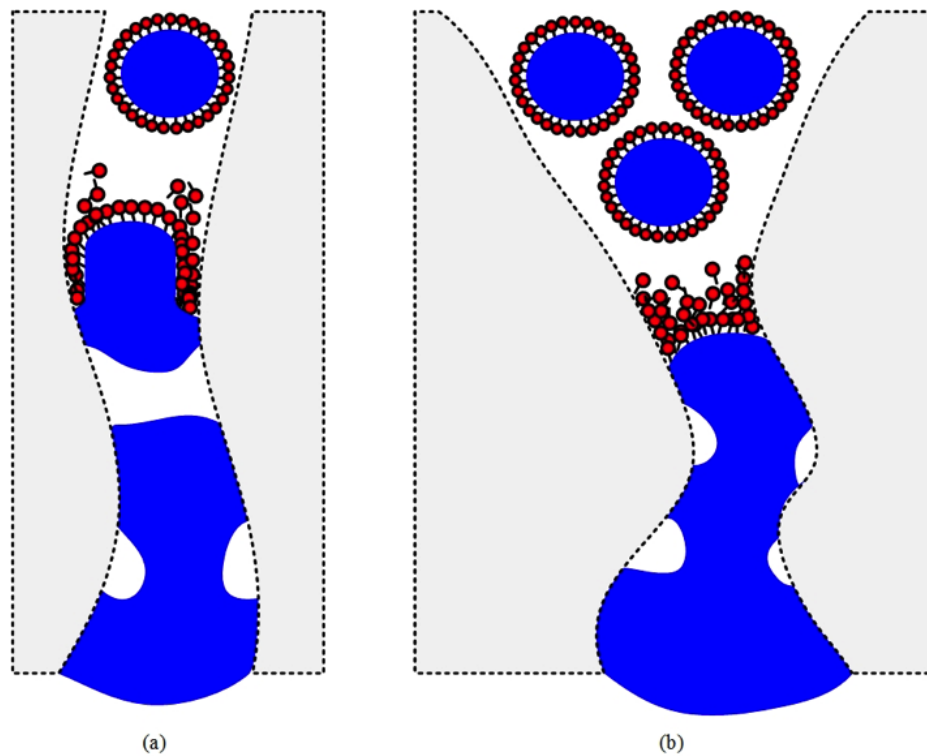


Figure 7 The coalescence of the oil droplets in the tortuous path of sponge-like structure membranes for the initial size of oil droplets smaller than the membrane surface pore size: (a) membrane surface with smaller pore size (b) membrane surface with larger pore size

4.0 CONCLUSIONS

PVDF membranes with sponge-like structure have been successfully fabricated by using phase inversion technique and coagulating in the water bath containing 30% v/v ethanol solution. Three types of membranes were formulated i.e. without additive (PVDF1), with water (PVDF2) and PEG1000 (PVDF3) as the additives in the dope solutions. The membrane thickness, porosity and pore size increased in the order of the membranes PVDF3>PVDF2>PVDF1. The additives in the dope solutions caused the membrane structures to become more porous, spongy and resilient. The PVDF3 membrane having the larger pore size range than the PVDF2 because the molecular weight of the PEG was larger than that of the water. With the larger pore size range and more open pore structure in the PVDF3 membrane, more oil droplets were trapped and coalesced to form larger oil droplets in the permeate.

ACKNOWLEDGEMENT

The authors gratefully acknowledge the financial support from the Ministry of Higher Education Malaysia under the Fundamental Research Grant Scheme (FRG0418-TK-1/2015).

REFERENCES

- [1] R. Fortenberry. 2013. Experimental demonstration and improvement of chemical EOR techniques in heavy oils. M.S Thesis, University of Texas at Austin.
- [2] G. Shutang, L. Huabin, Y. Zhenyu, M.J. Pitts, H. Surkalo, K. Wyatt. 1996. Alkaline/surfactant/polymer pilot performance of the West Central Saertu, Daqing oilfield. *SPE Reserv. Eng.* 11: 181–188.
- [3] V. Alvarado, E. Manrique. 2010. Enhanced oil recovery: An update review. *Energies* 3: 1529–1575.
- [4] Q. Qi, H. Gu, D. Li, L. Dong. 2000. The pilot test of ASP combination flooding in Karamay oil field. In: Paper SPE 64726 presented at the 2000 SPE International Oil and Gas Conference and Exhibition in China, 7–10 November, Beijing.
- [5] T. Chen, G. Zhang, J. Ge, H. Yang. 2013. The research on weak alkali ASP compound flooding system for Shengli heavy oil. *Adv. Petrol. Explor. Dev.* 5: 106–111.
- [6] S.R. Clark, M.J. Pitts, S.M. Smith. 1993. Design and application of an alkaline-surfactant-polymer recovery system to the west Kiehl field. *SPE Adv. Technol. Series* 1: 172–179.
- [7] B. Seyler, J. Grube, B. Huff, N. Webb, J. Damico, C. Blakley. 2012. Reservoir characterization of Bridgeport and Cypress sandstones in Lawrence field Illinois to improve petroleum recovery by alkaline-surfactant-polymer flood. *Ener. Technol. Data Exchange* 2012-12-21.
- [8] C.S. Gregersen, M. Kazempour, V. Alvarado. 2013. ASP design for the Minnelusa formation under low-salinity conditions: Impacts of anhydrite on ASP performance. *Fuel* 105: 368–382.
- [9] O.O. Foyeke, J.B. Diane. 1998. Influence of interfacial properties of lipophilic surfactants on water-in-oil emulsion stability. *J. Colloid Interf. Sci.* 197: 142–150.

- [10] A. Fakhru'l-Razi, P. Alireza, C.A. Luqman, R.A.B. Dayang, S.M. Sayed, Z.A. Zurina. 2009. Review of technologies for oil and gas produced water treatment. *J. Hazard. Mater.* 170: 530–551.
- [11] H. Unno, H. Saka, T. Akehata. 1986. Oil separation from oil-water mixture by a porous poly(tetrafluoroethylene) (PTFE) membrane. *J. Chem. Eng. Japan* 19: 281–286.
- [12] M. Hlavacek. 1995. Break-up of oil-in-water emulsions induced by permeation through a microfiltration membrane. *J. Membr. Sci.* 102: 1–7.
- [13] U. Daiminger, W. Nitsch, P. Plucinski, S. Hoffmann. 1995. Novel techniques for oil/water separation. *J. Membr. Sci.* 99: 197–203.
- [14] T. Kawakatsu, R.M. Boom, H. Nabetani, Y. Kikuchi, M. Nakajima. 1999. Emulsion breakdown: Mechanisms and development of multilayer membrane. *AIChE J.* 45: 967–975.
- [15] A. Hong, A.G. Fane, R. Burford. 2003. Factors affecting membrane coalescence of stable oil-in-water emulsions. *J. Membr. Sci.* 222: 19–39.
- [16] P. Sukitpaneemit, T.S. Chung. 2009. Molecular elucidation of morphology and mechanical properties of PVDF hollow fiber membranes from aspects of phase inversion, crystallization and rheology. *J. Membr. Sci.* 340: 192–205.
- [17] D. Wang, K. Li, W.K. Teo. 1999. Preparation and characterization of polyvinylidene fluoride (PVDF) hollow fiber membranes. *J. Membr. Sci.* 163: 211–220.
- [18] S.P. Deshmukh, K. Li. 1998. Effect of ethanol composition in water coagulation bath on morphology of PVDF hollow fiber membranes. *J. Membr. Sci.* 150: 75–85.
- [19] D. Hou, H. Fan, Q. Jiang, J. Wang, X. Zhang. 2014. Preparation and characterization of PVDF flat-sheet membranes for direct contact membrane distillation. *Sep. Purif. Technol.* 135: 211–222.
- [20] E. Saljoughi, M. Amirilargani, T. Mohammadi. 2010. Effect of PEG additive and coagulation bath temperature on the morphology, permeability and thermal/chemical stability of asymmetric CA membranes. *Desalination* 262: 72–78.